ELSEVIER

Computational Materials Science 9 (1997) 237–250

COMPUTATIONAL MATERIALS SCIENCE

Crystal spin in two-sites self consistent models: From kinematics to kinetics

R.E. Bolmaro [a,*], R.A. Lebensohn [a], H.-G. Brokmeier [b]

[a] *Instituto de Física Rosario, Fac. Ciencias Exactas, Ingeniería y Agrimensura, CONICET-UNR, Bv. 27 de febrero 210 bis., 2000 Rosario, Argentina*

[b] *Institut für Metallkunde und Metallphysik der Technische Universität Clausthal, Außenstelle am GKSS Forschungszentrum Geesthacht, Max-Plank-Str. 03, D-21502 Geesthacht, Germany*

Abstract

In the current presentation we deal with the interpretation of textures of two-phase co-deformable materials. We use a 2-sites visco plastic self consistent (2S-VPSC) model computing the spin of each phase through an empirical law describing spin sharing between both phases. Cu–Fe and Ag–Ni composite materials represent two kinds of two-phase materials that have been extensively studied in the past. Neutron and X-ray texture measurements of rolled, free compressed and extruded samples are shown and analyzed in light of the model. Many of the particularities shown by both materials are explained and a general discussion of the model is provided. © 1997 Elsevier Science B.V.

PACS: 62.20.Fe; 81.40; 82.20.wt
Keywords: Textures; Two-phase materials; Neutron diffraction; Self-consistent models

1. Introduction

Many different Self Consistent (SC) approaches have been used in the past for texture simulation in single [1,2] as well as in two-phase materials [3,4]. Most of those SC models have been implemented numerically in their 1-site approximation [5–8]. Those approaches amount to consider each grain as an inclusion embedded in a homogeneous equivalent medium having the average properties over the whole set of grains. This implies that the vicinity effects are neglected. It has been proven that this, somehow crude, assumption gives acceptable results for single phase materials [8]. However, in the case of two-phase materials a 2-sites, instead of a 1-site, approach has proven to be relevant to get improved results [4–9]. In multiphase materials, the vicinity effects may be relevant when the neighbor sites of different phases are crystallographically and/or morphologically correlated. For the 2S-VPSC Eshelby's solution of the 1-inclusion problem [10] is extended to the case of two interacting viscoplastic ellipsoidal inclusions embedded in a viscoplastic matrix that undergoes a macroscopic stress–strain rate state. The fundamental equations of the 2S-VPSC model have been summarized in Ref. [9] while a complete description can be found in Ref. [4]. We will deal here with a modification of the model, that will be described in the second section, and with its application

* Corresponding author. Tel.: +54-41-212028/853200/853222; fax: +54-41-821772/264008; e-mail: bolmaro@ifir.ifir.edu.ar.

PII S0927-0256(97)00079-7

to special model cases. Cu–Fe and Ag–Ni composite materials represent two kinds of two-phase materials well suited for modelization [2,11,12]. A brief on the experimental results will be presented in the third section. Neutron and X-ray texture measurements of rolled, free compressed and extruded samples are analyzed in light of the model in the fourth section.

2. The kinematics of spin

By far, a 2-sites SC model is an improvement over 1-site schemes in which the interaction of each grain has no preference for any of its neighbor grains. Nevertheless, the self consistent interaction scheme takes only into account the relative strength of each phase in two steps: firstly with its only nearest neighbor and secondly with an average matrix. The known interaction equation is established between the average stress and strain rate and the corresponding grain microscopic magnitudes. Certainly, the spin of each grain is not straightway related with its neighboring spin but only with the macroscopic spin of the whole test piece. Hereafter spin is meant to be the rate of rotation in the same way as strain rate is related with strain. A lot of information is lost about the spin of each grain because, among many reasons, the information about arrangement of grains in the material is not an input of the simulation. The relative rotation of grains around each other is strongly dependent on the interaction among them. That interaction has not been mathematically described until now.

In a 2-sites approach the way both grains share spins is dependent on at least the following factors:

(1) The crystal structure of both phases.

(2) The shape of both nearest neighbor grains.

(3) The texture or, better to say, the degree of development of it, of both phases.

(4) The strength of the interface in the sense of the tendency to fragment and/or deform inhomogeneously in the vicinities of the interface.

(5) Crystallographic correlation between phases.

(6) Volume fraction of both phases.

(7) Yield stress ratio between phases.

All those factors can influence one another. For instance, certainly the strength of the interface is a relative parameter. For well aligned, equally shaped and well-oriented grains the tendency of each grain to follow its companion must be strong. In the opposite case (round grains and randomly distributed orientations) the process of reorientation of grains can be energetically less expensive if grain fragmentation (inhomogeneous deformation) occurs. The grains will spin following their own needs to fulfill contiguity with an average matrix instead of strongly interact with their closest neighbors.

2.1. Basic assumptions of current models

The models available in the literature are characterized by dealing with large deformations through 'cumulative small deformation steps' or strain rates. In that scheme, strain rates and spins are separable which is not true in a real highly deformed material. However, the approach has proven to be accurate enough for texture simulations. The main assumptions, either in Taylor or self consistent approaches, are:

(i) The macroscopic strain rate is obtained as a weighted average over the microscopic strain rates of all grains

$$E = \sum_{k=1}^{n} \varepsilon^k / n = \langle \varepsilon^k \rangle \tag{1}$$

where E is the macroscopic strain rate tensor and ε^k is the microscopic strain rate tensor for each grain.

That assumption is trivially true for a Taylor model and self-consistently achieved by SC models.

(ii) For each grain it holds, step by step, that:

$$\Omega_{ij} = \Omega_{ij}^k = \Omega_{ij}^{k^*} + \Omega_{ij}^{k\mathrm{P}}, \tag{2}$$

where Ω_{ij}^k is the external macroscopic spin, assumed constant and equal to Ω_{ij} for every grain k, $\Omega_{ij}^{k^*}$ is the crystal system spin and $\Omega_{ij}^{k\mathrm{P}}$ is the spin of the grain shape due to plastic crystal slip.

That assumption hides a more general assumption about the average spin of all grains in the sample. That is to say that

$$\Omega_{ij} = \langle \Omega_{ij}^k \rangle = \langle \Omega_{ij}^{k^*} + \Omega_{ij}^{k\mathrm{P}} \rangle \tag{3}$$

what means that, essentially, even self consistent models use a Taylor like approach to spin sharing among grains. Even modern versions of SC models, which consider a local spin of the hole different for

each hole, do not consider, in the two-sites version, both coupled grains as a unique entity that has to fit that hole.

We will show by simple drawings how a more general approach can be obtained. We will carry out a schematic explanation of the model in the next paragraphs.

2.2. Sharing of spins

The present model holds under the assumptions of:

(i) The strain is homogeneous inside each grain.

(ii) The ratio among yield stresses is not high. Let us fix it between 1 to 3 to be arbitrary enough.

(iii) In consequence, there is no wrapping of one phase around the other by effect of the deformation. For instance, curling of one phase around the other is not covered by the current model. Modelization of bcc–fcc mixtures like Cu–Nb and Cu–Fe has to be taken with caution.

Those conditions seem to be not too restrictive because they are just natural extensions of the validity conditions of self-consistent models.

(i) One site approach to the spin problem

Each grain tries to fit inside a hole that is the ellipsoid left by the average strain rate and spin of the rest of the grains. Those holes are more or less aligned with the macroscopic shape of the sample and usually simulations based on single hole orientation, without considering local reorientations for each hole, are good enough for 1-site and 2-sites SC approaches (Fig. 1).

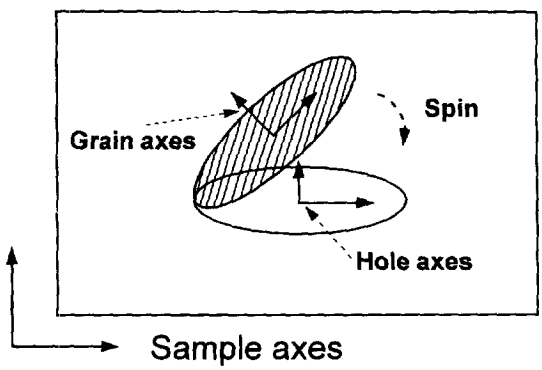

Fig. 1. Schematic drawing of the reorientation of a grain after deformation under the classical assumption: One grain fits its own hole.

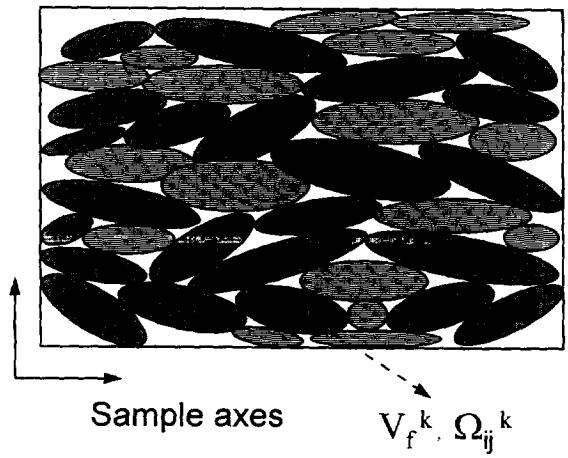

Fig. 2. Schematic depiction of the spatial orientation of grains in a polycrystal.

(ii) N-sites approach to the spin problem.

All the grains have deformed and spun in such way that the average strain rate coincides with the macroscopic one and the average spin coincides with the spin of the whole sample. For grains as the ones depicted in Fig. 2, under the conditions of 'no-wrapping' and not 'too-different' strain rates, the average for the spin is written:

$$\Omega_{ij} = \sum_k V_f^k \Omega_{ij}^k \tag{4}$$

(iii) 2-sites approach to the spin problem.

If the exact geometry and distribution of each grain are known, in some cases, we can consider that the grains can glide along the grain boundaries. In other words, in some special situations we can assume that there is no need for single grain spin, Ω^{k^*}, if two grains can complementary fit the two-grains hole that has been apportioned to them (Fig. 3a).

In some other cases, the grains behave pretty much the same as in the usual model of each grain fitting its own hole (Fig. 3b).

Many different situations can be imagined but all of them require the perfect knowledge of geometrical and topological features. The relative strain rates and spins between both grains are straight consequence of them.

A less detailed vision, always keeping in mind the conditions assumed in the beginning of the para-

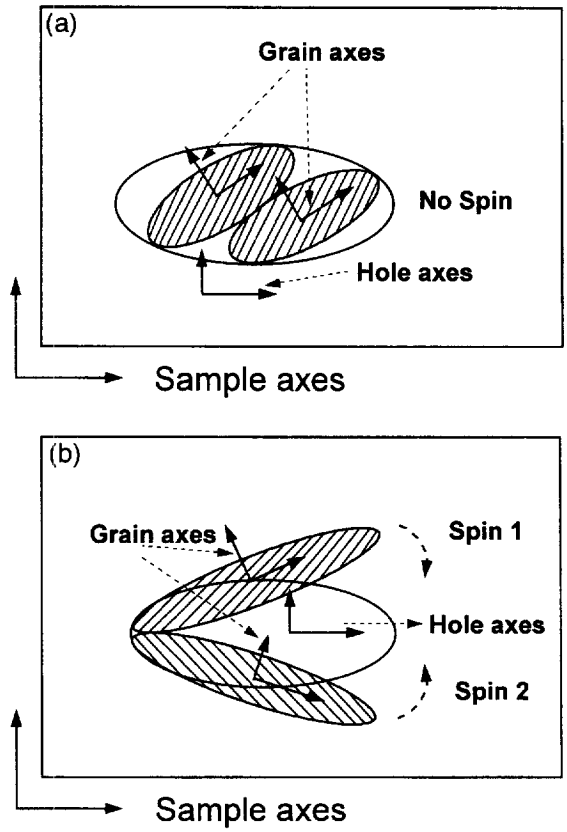

Fig. 3. Single hole–two grains mechanisms of reorientation. (a) Spin absent. Both grains fit the hole after deformation with no need of further spin. (b) Spin in coincidence with one hole–one grain model. Both grains must counter-spin to fill the original hole.

graph about strain rates and spins, will be worked out in the following. Nevertheless, the model will become operative in that way.

Let us write the Eq. (3) for just two grains of equal volume

$$\Omega_{ij} = \langle \Omega_{ij} \rangle = \left(\Omega_{ij}^{1^*} + \Omega_{ij}^{2^*} + \Omega_{ij}^{1P} + \Omega_{ij}^{2P} \right)/2 \quad (5)$$

where $\langle\ \rangle$ means the average magnitude. If the average spin $\langle \Omega_{ij}^{*} \rangle$ is associated with the spin of the 'average hole' apportioned to each pair of grains, then

$$\langle \Omega_{ij}^{*} \rangle = \left(\Omega_{ij}^{1^*} + \Omega_{ij}^{2^*} \right)/2 = \Omega_{ij} - \left(\Omega_{ij}^{1P} + \Omega_{ij}^{2P} \right)/2 \quad (6)$$

and we should use an average grain shape spin (produced by the plastic deformation), for both grains, subtracted from the macroscopic spin. The direct consequence is that both grains in a 2-sites SC approach will keep constant relative orientation. This must be true after a certain amount of deformation when the grains are *well aligned, well deformed and well oriented.* The question is how much is well aligned, well deformed and well oriented. Certainly it does depend on volume fraction of both species, relative strength (yield stress ratio), etc. The kinetics of the reorientation problem, stemming from the current kinematical description, will become evident in the next sections.

In the fourth section of the paper we will present some simulations made by using 1-site and 2-sites approaches. In this last case we will show some results using different assumptions about the amount of dragging effect each phase is producing over the other one. Moreover, in a real two-phase composite, percolation should play a paramount role in the behavior of each material. We will deal with that geometrical phase transition, and different behavior of phases, by using a physically based 'ad hoc' hypothesis about strain rate sensitivity of both phases.

3. Experimental results

The experimental results will be a collection of previously published results plus new ones [2,12]. The new ones were obtained by neutron diffraction mainly with the purpose of confirmation of some previously existent data. In multi-phase materials two effects can obscure the texture results obtained

Fig. 4. Inverse pole figures of Ag–Ni samples for an equivalent Von Mises deformation of 1.3 in free compression (a) 25%Ag–75%Ni, (b) 50%Ag–50%Ni, (c) 75%Ag–25%Ni.

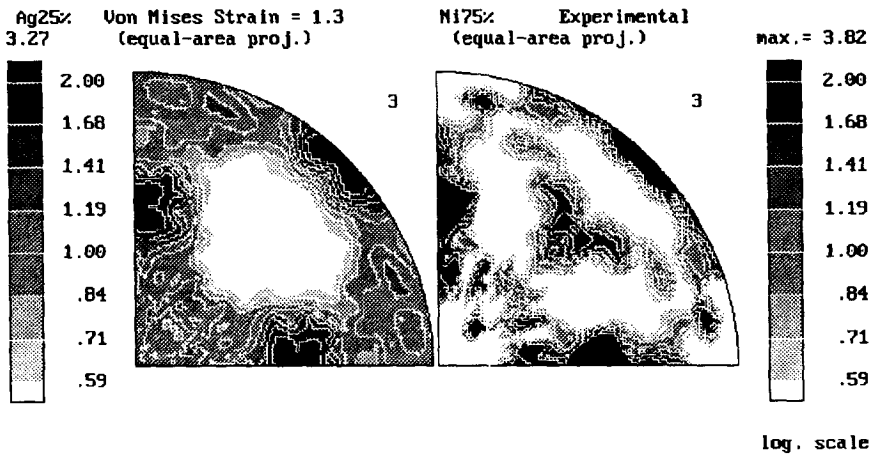
Ag25% Von Mises Strain = 1.3
3.27 (equal-area proj.)
Ni75% Experimental
(equal-area proj.)
max.= 3.82
2.00
1.68
1.41
1.19
1.00
.84
.71
.59
3
3
log. scale

a)

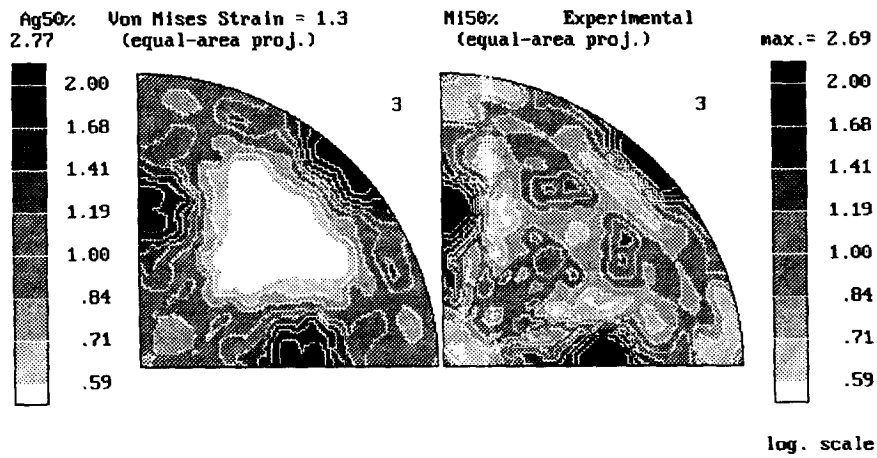
Ag50% Von Mises Strain = 1.3
2.77 (equal-area proj.)
Ni50% Experimental
(equal-area proj.)
max.= 2.69
2.00
1.68
1.41
1.19
1.00
.84
.71
.59
3
3
log. scale

b)

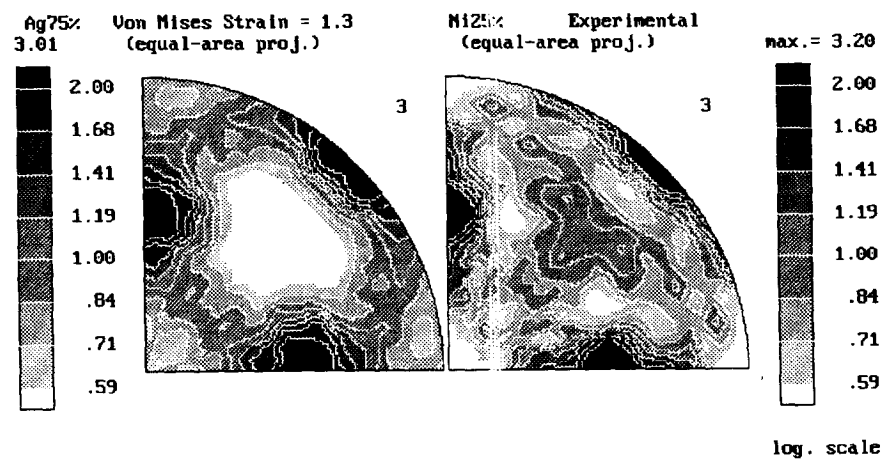
Ag75% Von Mises Strain = 1.3
3.01 (equal-area proj.)
Ni25% Experimental
(equal-area proj.)
max.= 3.20
2.00
1.68
1.41
1.19
1.00
.84
.71
.59
3
3
log. scale

c)

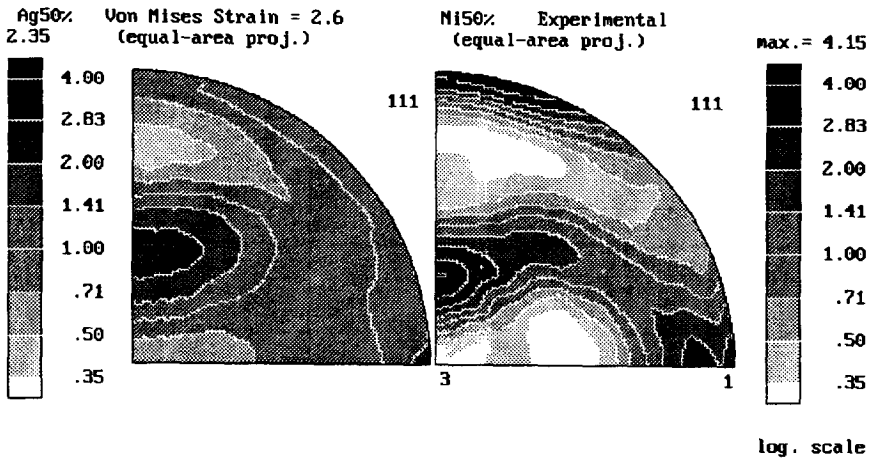

Fig. 5. Ag (111) and Ni (111) pole figures for 50%Ag–50%Ni after rolling at Von Mises equivalent strain of 2.6.

by X-ray diffraction: anisotropic absorption and peak overlapping. Anisotropic absorption is completely negligible in neutron techniques. Overlapping of peaks can be easily overcome by going to a higher index due to the constant atomic scattering factor of neutrons that allows to go to high angle reflections. Also, the high penetration depth of neutrons makes them a superb tool for texture measurements, in terms of statistics, on low textured materials. The typical sample volume of a neutron specimen is 1–4 cm^3. Lower volumes (approximately 0.1 cm^3) were measured with high accuracy at the research reactor FRG-1 at Geesthacht using the neutron texture diffractometer TEX-2 machine, due to its characteristic very low background.

3.1. Ag–Ni free compressed and rolled samples

The Ag–Ni samples were previously tested samples [2,9]. 25%Ag–75%Ni, 50%Ag–50%Ni and 75%Ag–25%Ni samples prepared by powder metallurgy techniques had been deformed by free compression and rolling to equivalent Von Mises strains of 1.3 and 2.6, respectively. The textures had already been measured by X-ray diffraction [2]. The very low intensities showed by almost all the compositions and mechanical tests suggested confirmation by neutron techniques.

3.2. Cu–Fe extruded samples

The samples were prepared by powder metallurgy. The starting materials were pure powders. On the one hand spherical iron particles of 13 μm average size and on the other hand dendritic copper powder of which the fraction < 32 μm was used [13]. Sample preparation starts with homogeneous mixing of volume fractions 75%Fe–25%Cu, 50%Fe–50%Cu and 25%Fe–75%Cu in a turbula mixer. Thereafter cylinders of 75 mm in diameter are compacted, heated up to 850°C and extruded to rods of 19.8 mm in diameter. The final state was obtained by cold drawing to deformation degrees of 63.5, 86.5, 95.1 and 98.2%. In addition pure iron and pure copper were processed identically to be able to compare with the rod composites.

3.3. Pole figure measurement

From each Ag–Ni sample the pole figures Ag (111), Ag (200), Ag (220), Ni (111), Ni (200) and Ni (311) were measured. It should be noticed that there is an almost complete overlap of Ag (200) and Ni (111). Calculation of the orientation distribution

Fig. 6. Experimental inverse pole figures for Cu–Fe powder composites after extrusion at Von Mises equivalent strain of 2.0. (a) 25%Cu–75%Fe, (b) 50%Cu–50%Fe, (c) 75%Cu–25%Fe.

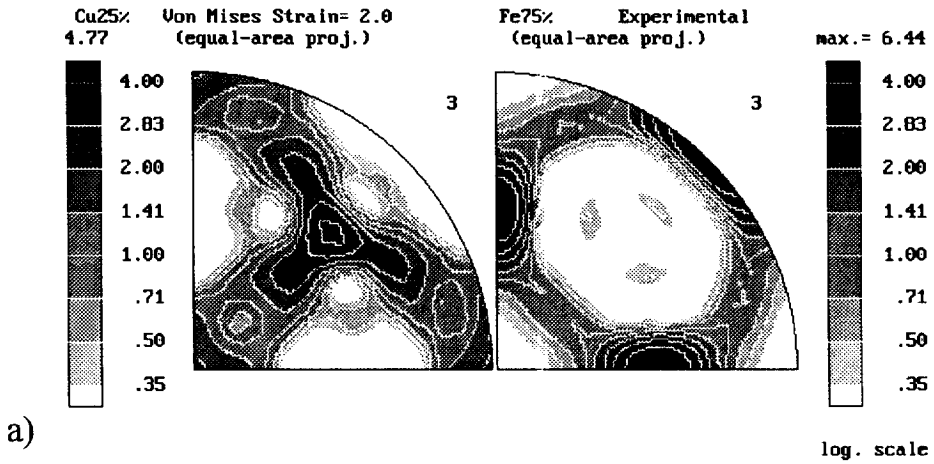
Cu25% Von Mises Strain= 2.0
4.77 (equal-area proj.)
Fe75% Experimental
(equal-area proj.)
max.= 6.44
4.00
2.83
2.00
1.41
1.00
.71
.50
.35
3
3
log. scale

a)

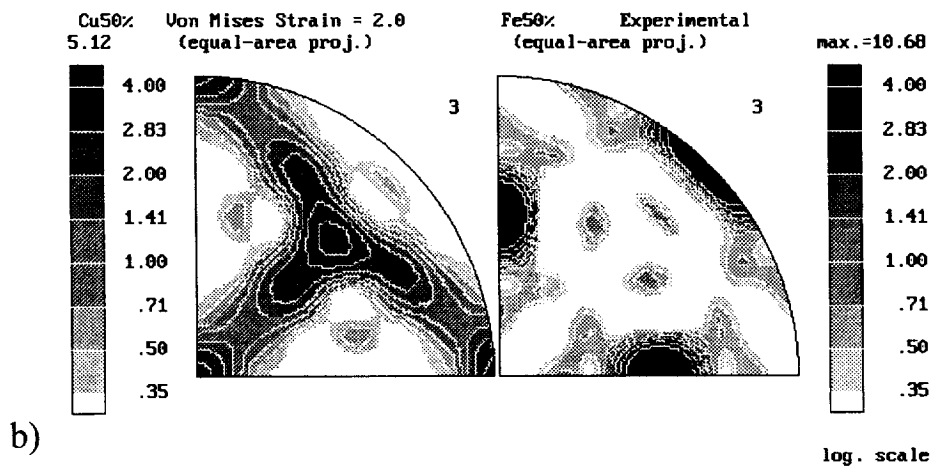
Cu50% Von Mises Strain = 2.0
5.12 (equal-area proj.)
Fe50% Experimental
(equal-area proj.)
max.=10.68
4.00
2.83
2.00
1.41
1.00
.71
.50
.35
3
3
log. scale

b)

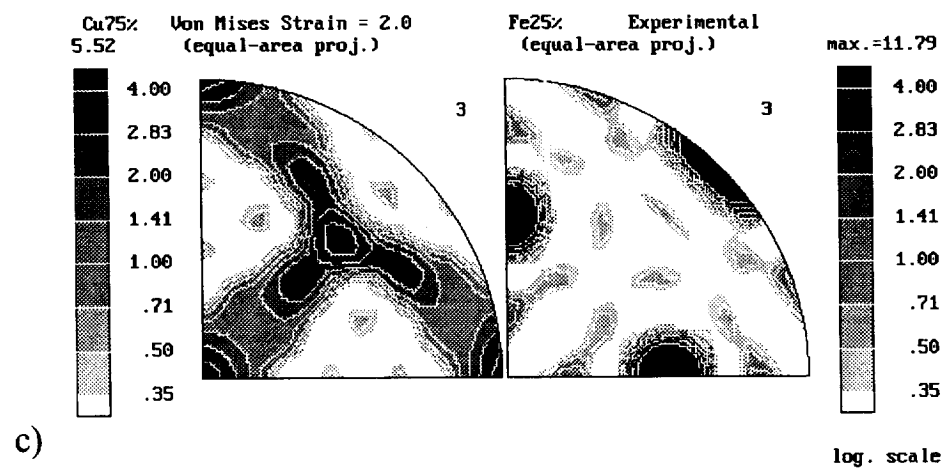
Cu75% Von Mises Strain = 2.0
5.52 (equal-area proj.)
Fe25% Experimental
(equal-area proj.)
max.=11.79
4.00
2.83
2.00
1.41
1.00
.71
.50
.35
3
3
log. scale

c)

function was carried out by the iterative series expansion method [14] which permits quantitative texture analysis in the case of multiphase materials with overlapping reflections [15]. The textures were also processed and further analyzed by using a PC-based package, popLA [16]. No significant differences were obtained by using both approaches.

The inverse pole figures of the three compositions of Ag–Ni samples, measured by X-ray diffraction, are shown in Fig. 4(a–c) for an equivalent Von Mises deformation of 1.3 in free compression. Fig. 5 shows the Ag (111) and Ni (111) pole figures obtained by neutron diffraction from the rolled sample at Von Mises equivalent deformation of 2.6. All textures measured by neutron diffraction compare well with the ones obtained by X-ray measurements although the first ones present better defined contours due to better statistics. Also, an orthotropic symmetry was revealed in the free compression samples. That symmetry was hidden by the low accuracy of X-ray methods when the textures are not well developed and the phenomena of peak overlapping and anisotropic absorption are present. In fact a non-well-developed Ni (111) component present in the textures measured by X-rays can be assumed to be consequence of the orthotropic symmetry and anisotropic absorption effects. The orthotropic symmetry stems from the square shape of the samples tested under free compression. Although the test was, in principle, cylindrically symmetric the friction between the sample and machine tools might have prevented a real cylindrically symmetric fibre texture development. This effect will be discussed in a coming paper [17].

From each CuFe sample the pole figures Cu (111), Cu (200), Cu (220), Fe (110), Fe (200) and Fe (211) were measured. Due to the highly symmetric deformation the pole figures show rotational symmetry. Thus only a low number of pole figures were measured completely.

In order to reduce the counting time the high symmetry was taken into account and α-scans were measured. An α-scan represents a cross section through the pole figure and only steps of 5° tiltings are necessary.

It should be noticed that a partial overlap of Fe (110) and Cu (111) is present. The same analysis software as applied to the Ag–Ni system was used in this case [14–16]. Fig. 6(a–c) show the experimental inverse pole figures for the three different compositions.

4. Simulations

The simulations were carried out on different volume fractions and mechanical test situations. The best physically based and understandable fittings were obtained by assuming a 50%–50% average sharing of the crystal system spin Ω^{k*} (see Eq. (6)) between the closest neighbor grains and different stress exponents for the microscopic constitutive equation. The model takes care of different volume fractions of phases by assigning proportional volumes to companion crystals. By assuming a 50%–50% sharing of spins we assume to have some of the majority phase grains pared with its own phase for spin sharing purposes.

In the case of the Ag–Ni textures the relative strengths of both phases were parametrized by a starting yield stress for the harder phase (i.e., the nickel) of twice the yield stress of the softer one, taken arbitrarily equal to 1. Common FCC {111} ⟨110⟩ yield behavior was assumed for both phases. Microscopic strain hardening was assumed linear with slopes of 1.5 for Ag and 2 for Ni in the same arbitrary units used for critical stresses. Due to the codeformation process the average strain rate sensitivity showed by both phases is very high. Other than stress exponents indicative of the relative compliance of both phases, also an interaction factor is needed to take care of the relative compliance of the average matrix and the pair of closest grains [18]. A discussion of this aspect of the simulation is presented in Section 5. For the 25%Ag–75%Ni composite we used stress exponents equal to 9, 5 and 7 for the Ag,

Fig. 7. Simulated inverse pole figures for Ag–Ni powder composites under free compression at Von Mises equivalent deformation of 1.3. a) 25%Ag–75%Ni, b) 50%Ag–50%Ni, c) 75%Ag–25%Ni.

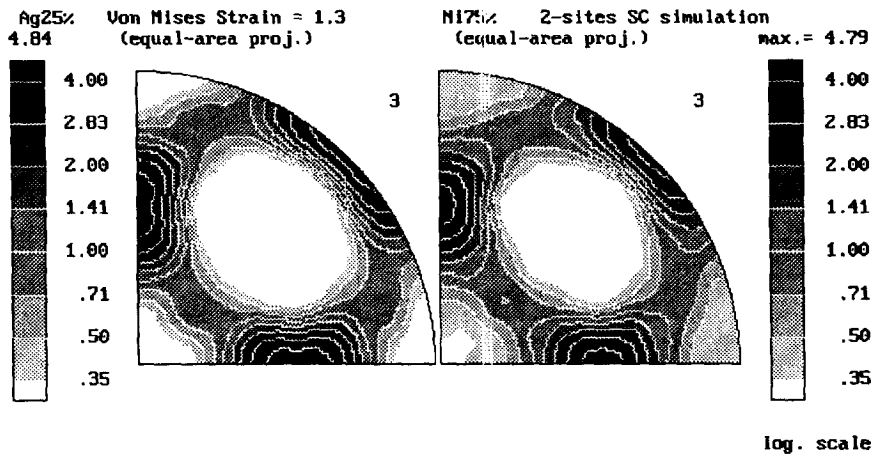
Ag25% Von Mises Strain = 1.3
4.84 (equal-area proj.)
Ni75% 2-sites SC simulation
(equal-area proj.)
max.= 4.79
4.00
2.83
2.00
1.41
1.00
.71
.50
.35
3
3
4.00
2.83
2.00
1.41
1.00
.71
.50
.35
log. scale

a)

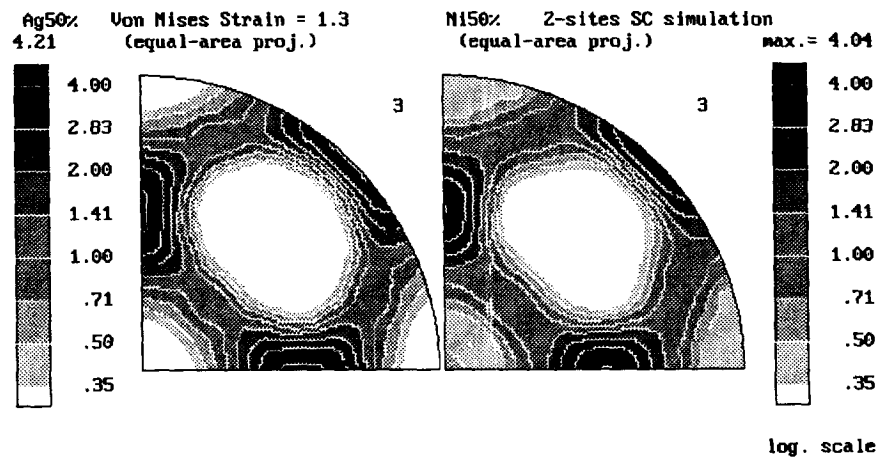
Ag50% Von Mises Strain = 1.3
4.21 (equal-area proj.)
Ni50% 2-sites SC simulation
(equal-area proj.)
max.= 4.04
4.00
2.83
2.00
1.41
1.00
.71
.50
.35
3
3
4.00
2.83
2.00
1.41
1.00
.71
.50
.35
log. scale

b)

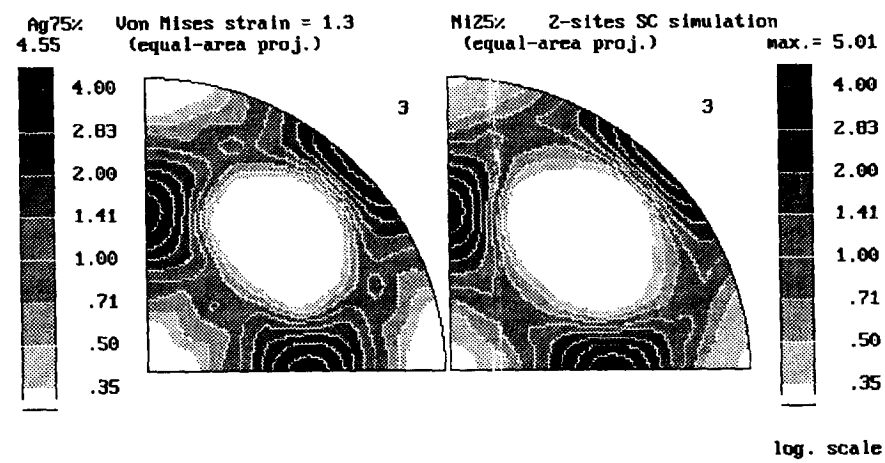
Ag75% Von Mises strain = 1.3
4.55 (equal-area proj.)
Ni25% 2-sites SC simulation
(equal-area proj.)
max.= 5.01
4.00
2.83
2.00
1.41
1.00
.71
.50
.35
3
3
4.00
2.83
2.00
1.41
1.00
.71
.50
.35
log. scale

c)

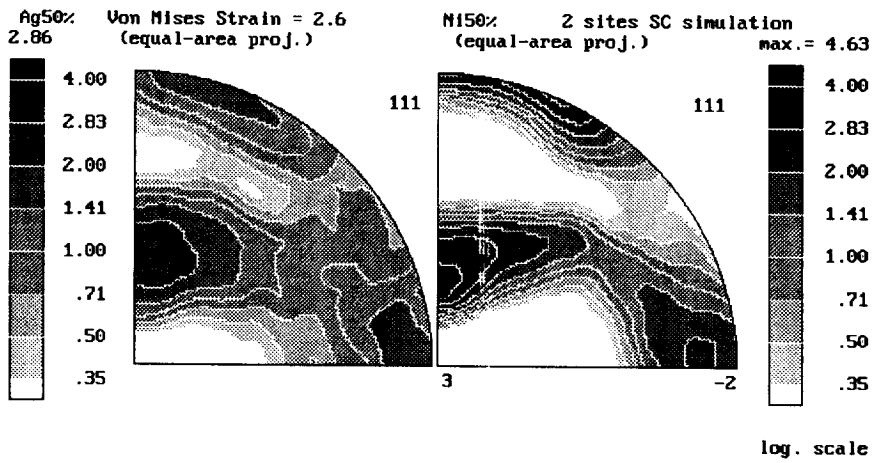

Fig. 8. Simulated Ag(111) and Ni(111) pole figures for 50%Ag–50%Ni under rolling conditions at Von Mises equivalent deformation of 2.6.

and Ni stress exponents and the interaction factor, respectively. For the 50%Ag–50%Ni composite all three stress exponents were taken equal to 5. For the 75%Ag–25%Ni composite we used $n = 5$, 9 and 7, respectively. Nevertheless, experimental observations show that Ag behaves as a viscous fluid flowing around the Ni particles for a broad variation of volume fractions [2,11]. That behavior suggested to use very different exponents for each phase for the case of rolling tests. We assigned a stress exponent of 5 to the Ag phase and a higher stress exponent of 33 to the Ni phase. The Ag behaved more 'viscous like' than the Ni phase. Those extreme values, necessary to explain the rolling behavior, may be consequence of the high constraint imposed by a rolling test.

The simulation is shown in Fig. 7(a–c) for the three different volume fractions deformed under free compression as inverse pole figures and in Fig. 8 for 50%Ag–50%Ni under rolling conditions as the Ag (111) and Ni (111) pole figures. With the current assumptions about strain rate sensitivities, yield stress ratio and strain hardening, the intensities are in fairly good agreement with the ones experimentally obtained for each phase at different deformations and volume fractions.

Fig. 9(a–c) show the simulated inverse pole figures obtained for the three different volume fractions of Cu–Fe composites. The iron was considered to be harder than the copper. The calculations were performed under the assumption of equal spin sharing. A final equivalent Von Mises deformation of 2.0 in extrusion was achieved in order to compare with the experimental values. That corresponds to an 86% reduction in area. We considered 500 grains randomly oriented and randomly related in pairs with other 500 grains of the other phase. The relative strengths of both phases were parametrized by a starting yield stress for the harder phase (i.e., the iron) of twice the yield stress of the softer one, taken arbitrarily equal to 1. Common FCC {111} ⟨110⟩ and BCC {110} ⟨111⟩ yield behaviors were assumed for Cu and Fe, respectively. Strain hardening was assumed linear with slopes of 1.5 for Cu and 2 for Fe in the same arbitrary units used for critical stresses. For the viscoplastic microscopic equation we assumed a stress exponent of 19 for both phases for 50%Cu–50%Fe, 27 for Cu and 11 for Fe for 25%Cu–75%Fe and 5 for Cu and 33 for Fe for 75%Cu–25%Fe. A coefficient of 19 was assumed for the interaction between both phases in all cases. The inversion of the exponents used for Cu and Fe

Fig. 9. Simulated inverse pole figures for Cu–Fe powder composites under extrusion at Von Mises equivalent deformation of 2.0. (a) 25%Cu–75%Fe, (b) 50%Cu–50%Fe, (c) 75%Cu–25%Fe.

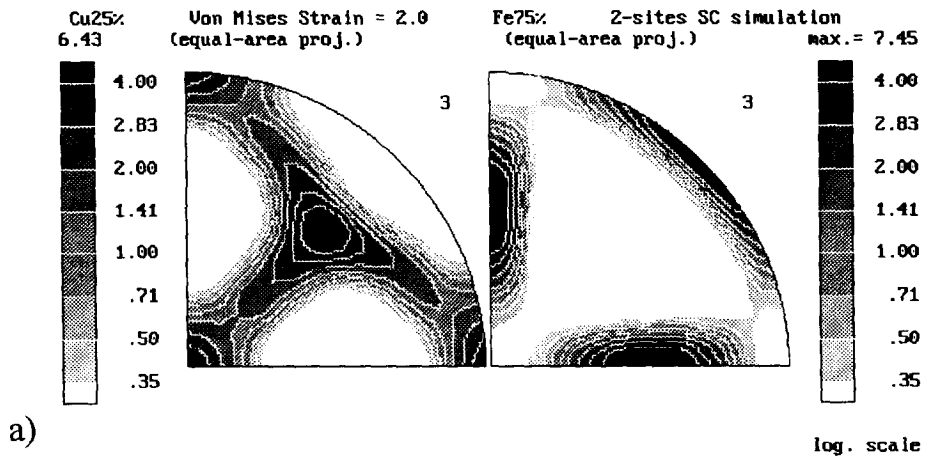
Cu25%
6.43
Von Mises Strain = 2.0
(equal-area proj.)
Fe75%
2-sites SC simulation
(equal-area proj.)
max.= 7.45
4.00
2.83
2.00
1.41
1.00
.71
.50
.35
3
3
log. scale

a)

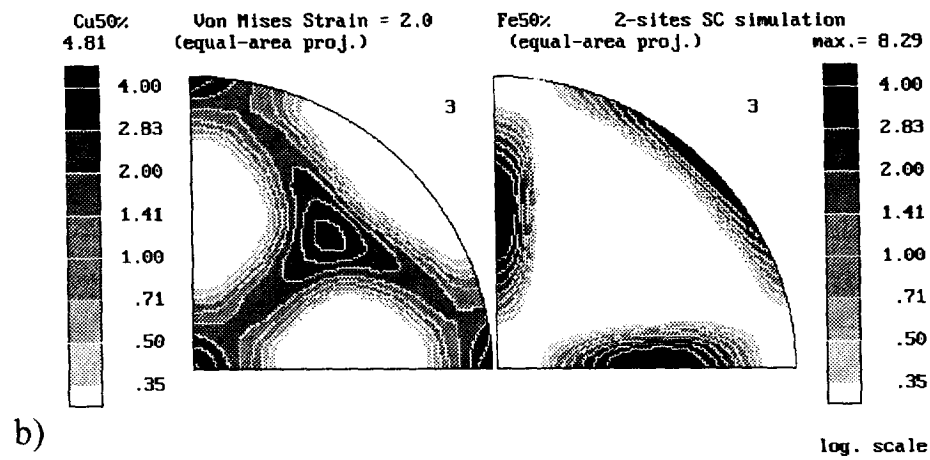
Cu50%
4.81
Von Mises Strain = 2.0
(equal-area proj.)
Fe50%
2-sites SC simulation
(equal-area proj.)
max.= 8.29
4.00
2.83
2.00
1.41
1.00
.71
.50
.35
3
3
log. scale

b)

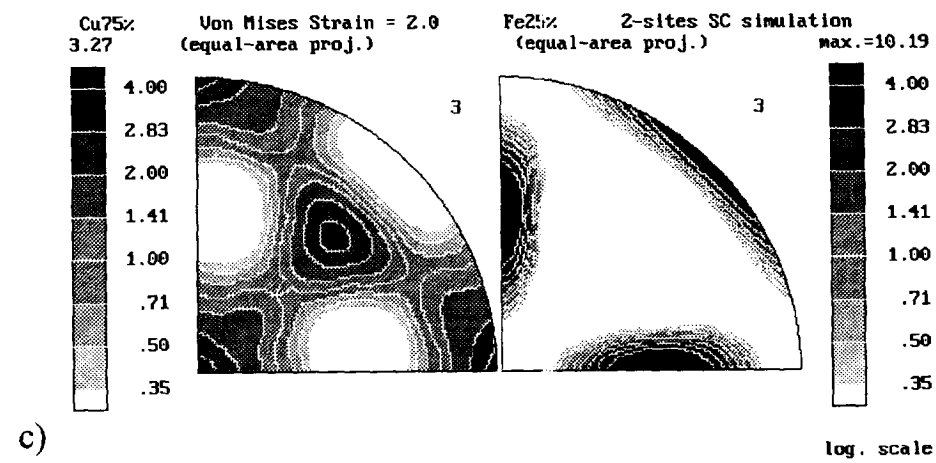
Cu75%
3.27
Von Mises Strain = 2.0
(equal-area proj.)
Fe25%
2-sites SC simulation
(equal-area proj.)
max.=10.19
4.00
2.83
2.00
1.41
1.00
.71
.50
.35
3
3
log. scale

c)

for the two extreme compositions stems from the different behavior assigned to those extreme volume fractions. Whichever the composition the minority phase behaves as isolated particles subject to small variations in the velocity gradient. The majority phase flows around those particles suffering more variation in the velocity gradient and acquiring a more viscous fluid behavior. By those assumptions we introduce empirically the place to place variation of the velocity gradient that can be observed in this kind of co-deforming metal–metal composites. Comparison between Fig. 6(a) and Fig. 9(a) (Cu25%–Fe75%) shows that finer adjustments of the proposed active slip systems or starting grain shapes are necessary to explain some component splitting in Cu. Also the 'curling effect' should be carefully considered in this kind of two-phase materials.

5. Discussion and conclusions

The commitment of the simulation was to achieve a coarse explanation of intensity levels of both phase textures. Small variations between different components were well beyond the scope of the research. For that reason the slip systems and/or possible combinations with twining systems have not been extensively investigated. Nevertheless, the close agreement obtained for the different experimental and simulated components of cubic textures allows to get some insights in the micromechanical behavior of both phases. The proposed sharing of spins seems to be in agreement with the experimental results. At least in the narrow range of volume fractions that goes from 25% to 75% and maximum yield stress ratio of 2. The scheme might be applicable to any simulation that considers phases with those characteristics. Nevertheless, the scheme should be confirmed by EBSP techniques, or any other local texture measurement. The relative orientation of both phases should be checked before and after deformation and it could be tracked for different deformation values. That information would be very valuable for the introduction of sharing parameters at different stages of the deformation process.

The variation of stress exponents is not meant to be a description of the real facts but only a physically based numerical trick to enforce different velocity gradient distributions for each phase. In a more detailed model (N-sites approach, FEM based models) that variation should come out naturally from the interaction equations between different grains and phases. In fact, previous calculations performed by Finite Element Models show the effect of strain path changes and fast changing relative spins that conform regions of altered flow patterns of different magnitudes [2]. When those variations are kept within narrow limits, like in co-deformable materials, the effect can be introduced by modifications of the strain rate sensitivities of both phases. Certainly, what has been called the interaction problem is matter of further research [19]. In the sense of having two materials deforming at different paces we can expect, on average, that the one that is taking the most of the deformation will do it by exhibiting a lower strain rate sensitivity. The condition of being 'harder' or 'softer' can come either from the single phase material properties or from the interaction produced by volume fraction or phase distribution. Two phases with similar yield stresses and strain hardening coefficients would behave differently whether one or the other is percolating. The interpretation of the model, when applied to the Cu–Fe system, is that the iron, while is a minority phase, will deform less than the copper. That means that the strain rate is lower and we should use higher strain rate sensitivity parameters for the iron phase when it is the minority phase. On the other hand, when the iron becomes the majority phase and percolates it will get a larger portion of the strain and it will behave as having a lower strain rate sensitivity. When the model is applied to Ag–Ni composites the Ag is always wrapping the more round Ni particles; even at large Ni contents. In that case the Ni is taking always a smaller share of the strain and acting as having a higher strain rate sensitivity. Although that assumption seems to be dependent on the boundary conditions imposed by each test. Highly constrained deformation paths, like rolling and 'channel die' tests, seem to impose different local behavior to the constituents and the softer phase flows always easily around the harder phase. Less constrained tests, like free compression, allow the components to flow freely and rotate around each other provided that the yield stress ratio is kept close to 1. That effect is made evident in the simulation by

using very low stress exponents. Also the variation of stress exponents is smaller for both phases in the case of free compressed Ag–Ni samples.

It is worthy to mention that by using different stress exponents for each phase we have been able to achieve degrees of matching between simulations and experiments unreachable by any other method. The increment of the number of parameters by itself could explain the ability of the model. Nevertheless, we should emphasize that the numerical values we found best agreeing with experiments are always rationalizable in terms of yield stress ratio, volume fraction, distribution of phases, etc.

For the purpose of quantification of the bondage of each sharing scheme, we calculated experimental and theoretical percentages of the different usual FCC ideal components after rolling, for the case of 50%Ag–50%Ni rolled material. The discrete orientations were supposed to belong to each component when they were in a cone of approximately 15° of the ideal components. In Table 1 we can observe the adjustment between simulations and experiments of the percentage represented by each component obtained for each degree of sharing of spins. We also show the average distance, expressed in radians, of the experimental or simulated orientations with respect to the ideal orientations. The different degrees of sharing of spins are obtained by using an interaction coefficient (denoted by ic in the Table 1) that allows different amounts of sharing. The ic parameter permits the spins to be shared between both phases in an amount proportional to the current deformation following some empirical law. The simulated values for each component at low deformation are indistinguishable from the experimental values of the Ag–Ni composite. Also a column with experimental data for pure Cu has been added. At high deformation the brass component of Cu is much lower and the S component percentage is higher than in the Ag–Ni composite. We can see that at low deformations (Von Mises equivalent strain of 0.65) the adjustment does not improve too much by considering any amount of sharing. At large deformations (Von Mises equivalent deformation of 2.6), when the grains have become well aligned and ellipsoidal, the adjustment is much better for the 50%–50% scheme. Except for the Goss component of Ni, the distribution of simulated components is in agreement with the experimental ones. Actually the agreement between simulations and Ag–Ni experiments is rather surprising. At low deformations it may be due to the fact that, even if sharing of spins is low, the spin itself is low because of the roundness of grains. At high deformations some of the simulated compo-

Table 1
Comparison among the relative development of different components for 1-site and 2-sites models and different sharing of spins. After rolling for different Von Mises strains

Von Mises strain = 0.65	1s		ic = 0.0		ic = 0.1		ic = 0.2		ic = 0.5		Exp.		Exp.
	Ag	Ni	Ag	Ni	Ag	Ni	Ag	Ni	Ag	Ni	Ag	Ni	Cu 1.1
Copper	8.8	11.4	7.8	8.2	7.0	9.0	7.2	9.2	6.6	10.6	9.3	9.4	8.9
Brass	14.0	15.0	17.4	16.0	13.2	12.0	11.0	9.8	8.8	9.8	4.3	5.3	6.2
S	9.8	14.4	10.2	16.0	11.0	10.4	12.6	12.6	12.4	10.4	10.0	9.8	15.9
Goss	10.8	12.4	9.8	10.8	8.6	11.8	8.8	10.0	6.0	8.4	3.2	3.8	3.4
Cube	1.0	0.6	1.6	0.6	2.0	1.2	2.0	1.0	2.2	1.6	3.3	2.7	4.8
Av.Dist	0.33	0.31	0.32	0.32	0.34	0.33	0.34	0.35	0.36	0.35	0.38	0.38	0.34
Von Mises Strain = 2.60	1s		ic = 0.0		ic = 0.1		ic = 0.2		ic = 0.5		Exp.		Exp.
	Ag	Ni	Ag	Ni	Ag	Ni	Ag	Ni	Ag	Ni	Ag	Ni	Cu 2.6
Copper	4.8	5.0	5.8	4.6	7.2	10.0	8.2	13.6	6.4	9.2	7.8	10.6	8.8
Brass	24.6	38.0	25.4	31.2	20.0	17.0	14.8	14.0	10.8	11.6	8.6	8.7	3.7
S	15.2	11.8	16.0	15.6	14.4	20.6	12.8	17.8	12.8	13.0	10.8	13.2	15.2
Goss	19.8	14.8	18.0	14.6	19.2	14.0	15.0	11.8	8.8	**11.2**	7.2	**3.4**	2.5
Cube	1.0	0.0	0.6	0.0	0.8	0.0	1.2	0.2	1.4	0.0	2.5	1.6	4.0
Av.Dist	0.26	0.25	0.26	0.26	0.28	0.28	0.31	0.30	0.35	0.33	0.36	0.35	0.35

nents are closer to the experimental ones when equal sharing of spins is allowed, improving even the results obtained by 2-sites simulations with low or no sharing of spins.

References

[1] G. Wassermann, H.W. Bergmann, G. Frommeyer, in: Proc. 5th. Int. Conf. on Textures of Materials, Vol II, Springer, Berlin, 1978, p. 37.
[2] R.E. Bolmaro, R.V. Browning, F.M. Guerra, A.D. Rollett, Mater. Sci. Eng. A 175 (1994) 113.
[3] G.R. Canova, H.-R. Wenk, A. Molinari, Acta Metall. 40 (1992) 1519.
[4] R.A. Lebensohn, G.R. Canova, Acta Mater., to be published.
[5] A. Molinari, G. Canova, S. Ahzi, Acta Metall. 35 (1987) 2983.
[6] E. Kröner, Acta Metall. 9 (1961) 155.
[7] J.W. Hutchinson, Proc. R. Soc. London A 348 (1976) 101.
[8] R.A. Lebensohn, C.N. Tomé, Acta Metall. 41 (1993) 2611.
[9] R.E. Bolmaro, R.A. Lebensohn, in: Proc. XI International Conference on Texture of Materials, Xi'an, China, 16–20 September, 1996.
[10] J.D. Eshelby, Proc. R. Soc. London A 241 (1957) 376.
[11] J.J. Petrovic, A.K. Vasudevan, Mater. Sci. Eng. 34 (1978) 39.
[12] H.-G. Brokmeier, Mater. Sci. Eng. A 175 (1994) 131.
[13] R. Beusse, W. Böcker, H.J. Bunge, Scr. Metall. 27 (1992) 767–770.
[14] M. Dahms, H.J. Bunge, J. Appl. Cryst. 22 (1989) 439–447.
[15] M. Dahms, H.-G. Brokmeier, H. Seute, H.J. Bunge, in: S.I. Andersen, H. Lilholt, O.B. Petersen (Eds.), Mechanical and Physical Behaviour of Metallic and Ceramic Composites, RISØ National Lab., Roskilde (DK), 1988, pp. 327–332.
[16] J.S. Kallend, U.F. Kocks, A.D. Rollett, H.-R. Wenk, Mater. Sci. Eng. A 132 (1991) 1–11.
[17] R.E. Bolmaro, H.-G. Brokmeier, to be published.
[18] M. Berveiller, A. Zaoui, C.R. 15°Colloque GFR, Paris, 1980, pp. 175–199.
[19] U.F. Kocks, Mater. Sci. Eng. A 175 (1994) 49–54.